Title
HIGH ENERGY PHOTO-NUCLEAR REACTIONS

Author
Strauch, Karl

Publication Date
1950-10-04

UNIVERSITY OF CALIFORNIA

Radiation Laboratory

BERKELEY, CALIFORNIA

DISCLAIMER

UCRL-708 Rev.
Unclassified Distribution

UNIVERSITY OF CALIFORNIA

Radiation Laboratory

Contract No. W-7405-eng-48

HIGH ENERGY PHOTO-NUCLEAR REACTIONS

Karl Strauch

October 4, 1950

Berkeley, California

INSTALLATION:	Number of Copies
Argonne National Laboratory	8
Armed Forces Special Weapons Project	1
Atomic Energy Commission - Washington	2
Battelle Memorial Institute	1
Brush Beryllium Company	1
Brookhaven National Laboratory	4
Bureau of Medicine and Surgery	1
Bureau of Ships	1
Carbide and Carbon Chemicals Division (K-25 Plant)	4
Carbide and Carbon Chemicals Division (Y-12 Plant)	4
Chicago Operations Office	1
Columbia University (J. R. Dunning)	1
Columbia University (G. Failla)	1
Dow Chemical Company	1
H. K. Ferguson Company	1
General Electric, Richland	3
Harshaw Chemical Corporation	1
Idaho Operations Office	1
Iowa State College	2
Kansas City Operations Branch	1
Kellex Corporation	2
Knolls Atomic Power Laboratory	4
Los Alamos Scientific Laboratory	3
Mallinckrodt Chemical Works	1
Massachusetts Institute of Technology (A. Gaudin)	1
Massachusetts Institute of Technology (A. R. Kaufmann)	1
Mound Laboratory	3
National Advisory Committee for Aeronautics	1
National Bureau of Standards	3
Naval Medical Research Institute	1
Naval Radiological Defense Laboratory	2
New Brunswick Laboratory	1
New York Operations Office	3
North American Aviation, Inc.	1
Oak Ridge National Laboratory	8
Patent Branch - Washington	1
RAND Corporation	1
Sandia Corporation	2
Santa Fe Operations Office	2
Sylvania Electric Products, Inc.	1
Technical Information Division (Oak Ridge)	15
Armament Division, Deputy for Research and Development (Capt. Glenn Davis)	1
Assistant for Atomic Energy, Deputy Chief of Staff (Col. Robert E. Greer)	1
Chief of Documents and Disseminations Branch (Col. J. E. Mallory)	1
USAF Assistant for Research Director of Research and Development Deputy Chief of Staff, Development (Colonel B. G. Holzman)	1
Electronic Systems Division (Mr. E. C. Trafton)	1
Chief of Scientific Advisors (Dr. Theodore Von Karman)	1
USAF, Eglin Air Force Base (Major A. C. Field)	1
USAF, Kirtland Air Force Base (Col. Marcus F. Cooper)	1

INSTALLATION:	Number of Copies
USAF, Maxwell Air Force Base (Col. F. N. Moyers)	1
USAF, NEPA Office	2
USAF, Offutt Air Force Base (Col. H. R. Sullivan, Jr.)	1
USAF Surgeon General, Medical Research Division (Col. A. P. Gagge)	1
USAF, Wright-Patterson Air Force Base (Rodney Nudenberg)	1
U. S. Army, Atomic Energy Branch (Lt. Col. A. W. Betts)	1
U. S. Army, Army Field Forces (Captain James Kerr)	1
U. S. Army, Commanding General, Chemical Corps Technical Command (Col. John A. MacLaughlin thru Mrs. Georgia S. Benjamin)	1
U. S. Army, Chief of Ordnance (Lt. Col. A. R. Del Campo)	1
U. S. Army, Commanding Officer, Watertown Arsenal (Col. Carrowll H. Deitrick)	1
U. S. Army, Director of Operations Research (Dr. Ellis Johnson)	1
U. S. Army, Office of Engineers (Allen O'Leary)	1
U. S. Army, Office of the Chief Signal Officer (Curtis T. Clayton thru Maj. George C. Hunt)	1
U. S. Army, Office of the Surgeon General (Col. W. S. Stone)	1
U. S. Geological Survey (T. B. Nolan)	2
U. S. Public Health Service	1
University of California at Los Angeles	1
University of California Radiation Laboratory	5
University of Rochester	2
University of Washington	1
Western Reserve University	2
Westinghouse Electric Company	4

Information Division
Radiation Laboratory
Univ. of California
Berkeley, California

UCRL-708 Rev.
Unclassified Distribution

HIGH ENERGY PHOTO-NUCLEAR REACTIONS

Karl Strauch

Radiation Laboratory and Department of Physics
University of California, Berkeley, California

October 4, 1950

Abstract

Transition curves in lead of the photons responsible for various nuclear reactions have been obtained using 322 Mev bremsstrahlung from the Berkeley synchrotron. The area under these curves or "track length" determines an effective photon energy, and the results are given in Table II. The integrated cross sections of the reactions $C^{12}(\gamma,n)C^{11}$ and $Cu^{63}(\gamma,n)Cu^{62}$ are found to be 0.090 and 0.76 Mev-barn respectively. Relative yields of various reactions from Zn have been measured, and relative cross sections have been calculated from these and the effective photon energies. A lower limit of 1.4 Mev-barns is obtained for the total cross section for photon absorption by the Zn nucleus, and 30 Mev is found for a lower limit to the average photon energy absorbed by the same nucleus. These results are discussed with respect to the proposed theories for nuclear photon absorption.

HIGH ENERGY PHOTO-NUCLEAR REACTIONS

Karl Strauch

Radiation Laboratory and Department of Physics
University of California, Berkeley, California

October 4, 1950

I. Introduction

With the development of high energy electron accelerators, x-ray beams have become available which contain photons energetic enough to produce multiple nuclear disintegrations. It is of interest to know the energies of the photons responsible and the cross sections for various reactions. These two quantities are difficult to obtain due to the continuous energy spectrum of the available bremsstrahlung. Baldwin and Klaiber[1] used the 100 Mev General Electric betatron to obtain excitation curves for the reactions $C^{12}(\gamma,n)C^{11}$, $Cu^{63}(\gamma,n)Cu^{62}$, U(γ,fission) and Th(γ,fission) by measuring the yield as a function of the electron beam energy and normalizing the beam intensity with the help of the calculated energy response of a monitor. Their results show a very narrow peak for the energy distribution of the photons responsible for the reaction under study, hereafter called "effective photons." McElhinney et al.[2] have obtained partial excitation functions for the reactions $Ta^{181}(\gamma,n)Ta^{180}$ and $Cu^{63}(\gamma,n)Cu^{62}$ by a similar method using the 21 Mev Illinois betatron. They find a greater spread in energy of the cross section peaks than do Baldwin and Klaiber; however, the "effective photons" are still well grouped around an average value. Similar results have recently been reported by Katz et al.[3]

---

[1] G. C. Baldwin and G. S. Klaiber, Phys. Rev. 70, 259 (1946); 71, 3 (1947); 73, 1156 (1948)

[2] J. McElhinney, A. O. Hanson, R. A. Becker, R. F. Duffield and B. C. Diven, Phys. Rev. 75, 542 (1949)

[3] L. Katz, H. E. Johns, R. A. Douglas and R. S. H. Haslam, Bull. Am. Phys. Soc. 25, No. 4, p. 16 (1950)

The conclusion that no very high energy quanta participate in these reactions is verified by the absolute cross section measurements on C by Lawson and Perlman[4] who obtain the same values with 50 Mev and 100 Mev bremsstrahlung. In addition, the relative yields of several reactions on many elements as obtained by Perlman and Friedlander[5] are found to be the same when measured with the 50 Mev and 100 Mev betatron beam.

With the completion of the Berkeley 322 Mev synchrotron, another approach to this problem became possible. By studying the intensity variation in an absorber, such as lead, of those photons responsible for a given nuclear reaction, it is possible to determine a mean energy value for these photons and to gain some information on their energy spread. This method will be studied and applied to several photonuclear reactions in Part II of this paper, and some relative and absolute cross section measurements will be described in Part III. The required theoretical calculations from the cascade shower theory are reported by L. Eyges in an accompanying paper.[6]

II. Transition Curves

A. Method. As the synchrotron beam passes through an absorber, its energy spectrum is changed by cascade processes: lower energy photons multiply, higher energy photons disappear. To study this transformation, detectors sensitive to various photon energies are required; these are available in the form of photonuclear reactions from different target nuclei. As we have just seen there is good evidence that the energies of the photons responsible for such reactions are grouped

---

[4] J. L. Lawson and M. L. Perlman, Phys. Rev. 74, 1190 (1948)

[5] M. L. Perlman and G. Friedlander, Phys. Rev. 74, 442 (1948); 75, 989 (1949)

[6] L. Eyges, Phys. Rev. (to be published)

in a narrow interval. The reaction is determined by the known target and product nuclei; the latter are identified by their radioactivities.

The amount of target activity is proportional to the number of photons responsible for the production of the radioactive product nucleus; thus, by placing identical targets at various depths in a lead absorber and comparing the induced activity, the density of "effective photons" is measured as a function of absorber thickness. The resulting curves are similar to the transition curves or Rossi curves obtained in cosmic ray work except that here the transformation in lead of a selected energy band of x-rays is being studied.*

We are primarily interested in the effective photon energy W_e responsible for various reactions; Eyges[6] shows that this can best be obtained from the area under the corresponding transition curve or its "track length." In the case of lead he obtains a simple analytic expression for W_e which is applied to the track length of the curves observed in this work. Some information on the accuracy of shower theory calculations in the energy region under consideration is also gained. This feature is examined in detail by Eyges.[6]

B. Experimental Apparatus and Procedure. In the normal set-up, hereafter designated Geometry 1, a stack of lead absorbers 9 x 9 inches in area was placed at 5 1/3 feet from the synchrotron Pt target (Fig. 1). The lead was of commercial grade and the measured surface density was divided by 6.5 gr/cm^2 to obtain the thickness in radiation lengths.** Foils of the target material had an area of

---

* In an attempt to measure threshold energies, Baldwin and Klaiber[1] have reported two such curves taken with the 100 Mev betatron beam.

**The value of 5.9 gr/cm^2 given by Rossi and Greissen[7] for the radiation length

[7] B. Rossi and K. Greissen, Rev. Mod. Phys. 13, 240 (1941)

3 3/4 x 3 3/4 inches and a thickness from 0.040 to 0.75 g/cm^2 determined by the activity required for counting purposes. The foils were mounted on thin cardboard holders and placed behind various thicknesses of lead. The whole stack was centered on the beam by the use of a telescope.

When a transition curve was measured for photons producing a short half-life such as Cu^{62}(10.1 minutes), a monitor foil was placed in front of the absorber stack and one or two foils placed inside during a run. At larger depths the induced activity becomes small; to be able to use longer bombardments, the monitor foil was then placed inside the stack at a previously measured position. If a longer half-life resulted from the reaction under study, e.g., Zn^{62} (9.5 hours), a complete set of 24 foils was placed inside the absorber stack during the irradiation.

After bombardment the foils were rolled into cylinders having a diameter of 7/8 inch, placed over Eck and Krebs thin-walled glass Geiger counters, and their activities compared. The consecutive interchange of samples compensated for the different counter efficiencies. In some cases, such as with Zn detectors, several half-lives are produced. Decay curves were then taken for each sample and the different product activities separated. The irradiation time depends, of course, on the half-life and the yield of the product activity, but

---

in Pb was increased 10 percent for the following reasons: The pair production cross section measurements by Lawson[8] and Walker[9] give results 10 percent lower than the theoretical calculations of Heitler.[10] Since bremsstrahlung and pair production are inverse processes to which detailed balancing applies, it is reasonable to assume that the radiation cross section is also 10 percent smaller than the theoretical values given in Heitler.[10]

[8] R. L. Walker, Phys. Rev. 76, 527 (1949)

[9] J. L. Lawson, Phys. Rev. 75, 433 (1949)

[10] W. Heitler, The Quantum Theory of Radiation (Oxford University Press, 1944)

it was in general of the same order as the half-life. A 2 mil Cu foil of standard size gives about 8000 counts per minute when placed in a 130 R/min beam as measured behind 1/8 in. lead at 1 meter from the target.

At the position of the lead stack the synchrotron beam has a width of about 1 inch between half intensity points; at 2 inches from the axis, the beam is down to 3 percent of its value at the axis. These results were obtained by comparing the activity of irradiated 1/4 inch diameter disks placed at various distances from the beam axis. The dimensions of Geometry 1 were chosen so as to include as much of the incident photon flux as practicable. Possible effects of scattering on the transition curves taken with this geometry will be examined in the following section.

The relative foil activity is plotted as a function of lead thickness in radiation lengths by normalizing the activity of the first foil to unity in all cases.

C. Influence of Geometry. As the x-ray beam passes through the lead stack it spreads in a lateral direction due primarily to multiple scattering of electrons. The quantitative interpretation of the transition curves depends on the applicability of one dimensional shower theory; this means that all the scattered photons must be detected.

The transition curve for the photons effective in the reaction $Cu^{63}(\gamma,n)Cu^{62}$ as obtained with Geometry 1 is shown by Curve 1 in Fig. 2. This transition curve was used to study the possible influence of scattering since it is due to lower energy photons for which such effects are expected to be most pronounced. The following tests were carried out:

(1) The transition curve was also taken using lead absorbers of area 2 1/2 x 3 1/2 inches and detector disks of 1 5/8 inches diameter; this is

Geometry 2 in Fig. 1. Standard end window Victoreen tubes were used to compare the activities. The results as shown by Curve 2 in Fig. 2 lie from 5 to 10 percent below the results obtained with Geometry 1. If we consider the difference in dimensions between the two geometries such a small difference in results indicates that scattering effects are not very important at these photon energies.

(2) The transition curves for photons effective in the reaction $C^{12}(\gamma,n)C^{11}$ obtained with Geometries 1 and 2 are identical. This is not suprising since the average energy of the photons responsible for this reaction is higher than for the previous one, and scattering is less important.

(3) To estimate the influence of the portion of the beam not usually effective, Geometry 3 (Fig. 1) was used; here monitor and detector foils are placed above their normal position so that only about 1 percent of the total beam is caught. The results are shown by Curve 3 of Fig. 2. If scattering outside Geometry 1 is important, more "effective photons" will scatter into Geometry 3 than out of it, resulting in a higher maximum than obtained under normal conditions. This is not observed; on the contrary, the peak is smaller as one would expect if it were primarily due to the outer edges of the synchrotron beam (there are proportionally fewer high energy photons in the outside portion of the beam). At larger depths Curve 3 appears to decrease less than normal. This is mainly due to neutron background which becomes appreciable at these low intensities. The transition curve obtained with Geometry 1 can be corrected using Curve 3 for the effect of the portion of the beam missing the detectors. Such corrections amount to 1 percent of the relative intensity which is smaller than other sources of error.

(4) To test for possible backscattering effects, Cu detector foils were placed at various positions in Geometry 1 with and without lead backing. No

significant difference in relative activity was observed.

(5) To determine whether the size of the beam had any influence on the shape of the transition curve, various collimators were used to cut the beam size down to 1/4 inch diameter. No change in peak height was observed.

The results of these tests indicate that the transition curves taken with Geometry 1 are not affected by the dimensions chosen. This means that the one dimensional shower theory can be applied.

The activity of the samples could also be produced by secondary electrons and neutrons present in the stack. The small cross sections for electron disintegrations measured by Laughlin et al.[11] show such contamination to be negligible, while the neutron background can be estimated from the behavior of the transition curves at larger absorber depths. The absorption coefficient for neutrons in Pb (about 0.1 per radiation length) is smaller than for photons. At large depths of lead, neutrons would be primarily responsible for the observed activities. In the curves reported here* the final absorption indicates small neutron background. It may be noted that the track length is quite insensitive to the behavior of the transition curves at large depths.

D. Results

Ag, Cu and C detectors. Short bombardments of silver, copper and polystyrene detectors result in activities produced primarily by (γ,n) processes: $Ag^{107}(\gamma,n)Ag^{106}$, 24 minutes (counting was started after the 2.3 minute activity of Ag^{108} had died out); $Cu^{63}(\gamma,n)Cu^{62}$, 10.1 minutes; $C^{12}(\gamma,n)C^{11}$, 20 minutes. In the first two cases these activities are also produced by $(\gamma,3n)$ reactions; the results

---

11 J. S. Laughlin, L. S. Skaggs, A. O. Hanson and J. J. Orlin, Phys. Rev. 73, 1223, (1948)

* The transition curve for the photons effective in the reaction $Al^{27}(\gamma,2pn)Na^{24}$ indicated a relatively large neutron background and is therefore not reported. In this case, the reaction cross section for x-rays is small, while the cross section for $Al^{27}(n,\alpha)$ is large.

reported in Part III indicate such contributions to be 3 percent or less. The transition curves for the photons effective in these three (γ,n) reactions as taken with Geometry 1 are shown in Figs. 3 and 4. In the case of Cu and C detectors, curves were obtained with bremsstrahlung with a maximum photon energy of about 200 Mev in addition to the 322 Mev maximum energy.

The five curves show the same characteristic features. As the synchrotron beam penetrates the lead stack, photons are absorbed. In the energy region of interest, the absorption is primarily due to pair production. The absorption of the "effective photons" originally present in the beam produces the initial dip of the transition curves. Some of the electrons produced by photons of energy much higher than W_e are responsible for the production of "effective photons" in one or more steps. This multiplication results in a rise or at least a levelling off of the transition curves. For a given beam energy, the rise is largest for the reaction with the lowest threshold (Ag). For a given detector the rise is smallest when the lower energy beam is used. At large depths multiplication of "effective photons" stops and an exponential absorption is approached. The slowest absorption is observed with the lowest threshold detector. The final slopes of the curves for the same detectors but different beam energies are the same within experimental error. Some of these features will be examined in more detail in Section E.

The values of W_e as obtained from the track length of these transition curves are given in Table II. The agreement with the results of McElhinney et al.[2] and Katz et al.[3] is good, but the results appear lower than would be expected from the excitation curves of Baldwin and Klaiber.[1] The ratio of the track lengths of the transition curves for "effective photons" of a given energy obtained with beams of different maximum photon energy is accurately predicted by shower theory since most approximations cancel out (see expression (9) in

Eyges' paper[6]). Theoretical and experimental results are presented in Table I; the agreement is satisfactory.

Long bombardments of Cu detectors allow the observation of the 12.8 hour product of the reaction $Cu^{65}(\gamma,n)Cu^{64}$. A few points of the corresponding transition curve were obtained and W_e estimated by comparison with the complete curves for (γ,n) processes.

Zn detectors. Fig. 5 shows transition curves for the photons causing several reactions from Zn and the corresponding values of W_e are given in Table II. The curves for the quanta responsible for the (γ,n), $(\gamma,2n)$, and (γ,pn) processes from Zn^{64} were obtained with Geometry 1. The observed activities have contributions of less than 10 percent from other Zn isotopes as seen in Part III. To obtain the transition curves for the photons responsible for the reactions $Zn^{64}(\gamma,p2n)Cu^{61}$, $Zn^{66}(\gamma,pn)Cu^{64}$, and $Zn^{68}(\gamma,p)Cu^{67}$, a special technique had to be used because of the low yield of the product activities. Thick detector foils (0.036 in.) were used, and the Cu products were separated with small amounts of carrier at the end of the bombardment; thus no sample self-absorption decreased the counting efficiency. This method did not prove practicable with the large foils of Geometry 1; instead 7/8 inch diameter disks were used in a stack placed at 2 1/3 feet from the synchrotron target. To correct for scattering of photons outside the detectors a transition curve with polystyrene detectors was taken and compared with the one obtained with Geometry 1. No difference was apparent up to 3 radiation lengths. Beyond that the required correction increased rapidly to 56 percent at 9 radiation lengths. Because of this large scattering only a few points were obtained for these curves; they serve to estimate W_e.

Ta detectors. Short bombardment in the 322 Mev synchrotron beam of Ta metal produces a new 70 minute half-life besides the 8 hour activity due to

$Ta^{181}(\gamma,n)Ta^{180}$. Chemical separations* have shown the short half-life to be associated with a rare earth; it is thus formed by the ejection of at least two charges. A few points of the transition curve of the photons responsible for this new activity are shown in Fig. 6. The high effective photon energy (Table III) obtained by assuming a straight line absorption curve, explains the absence of previous observation.

Long irradiation of Ta produces in addition several activities with a half-life of the order of days. These could not be separated from the 8 hour activity under the conditions of this experiment. Thus the transition curve shown in Fig. 6 is not produced by photons responsible only for the (γ,n) reaction, but also by quanta of higher energy. This is clearly shown by comparing its shape with the curve for the (γ,n) reaction in Cu. For absorber thicknesses of less than 5 radiation lengths, the Cu curve lies higher than the one for Ta, the reverse is true beyond that point. It is expected, therefore, that W_e = 19 Mev as obtained from the track length is too high.

Bi detectors. Bi disks of 2 7/8 inch diameter were used as detectors in Geometry 1 and many activities with half-lives ranging from minutes to days were observed after a three hour bombardment. It was not possible to resolve the decay curves into the various known half-lives in this region of the periodic table. The transition curve obtained at the end of the irradiation is shown in Fig. 6 and corresponds to very high energy photons. Two hours after the end of the bombardment, the transition curve became less steep, indicating that lower energy photons were producing the longer half-lives. The low activity of the samples when the effect became appreciable precluded quantitative observation.

Pb detectors. When Pb is irradiated with the 322 Mev beam, many activities appear besides the expected Tl^{206}(4 minutes) and Tl^{207} (5 minutes). As in

* The author is indebted to Dr. G. Wilkinson for carrying out this separation.

the case of Bi, the decay curves could not be resolved into half-lives known in this region. The curve shown in Fig. 6 for the "short half-lives" was taken 1 hour after the end of the bombardment and represents the relative sample activity for a period of 8 hours. After that time it began to rise slowly and the transition curve marked "long half-lives" was taken 36 hours after the end of the bombardment. The energies of the responsible photons as given in Table II represent lower limits only, due to the large neutron background in this case.

Further work, especially chemical separations, is being planned in the case of Bi and Pb to establish the origin of the new activities. It does not appear impossible that they are at least partially produced by photofission.*

E. Discussion. The transition curves presented here are caused by photons grouped in a certain energy range. What features of the curves are most energy sensitive? In the region under consideration, high energy photons are absorbed more rapidly than low energy quanta. The initial drop thus corresponds to the absorption of the photons participating in the reaction, averaged over the incident spectrum. It is difficult to measure this drop accurately since it is quite small (cf. Fig. 3). As can be seen from Fig. 1 in Eyges'[6] paper, the experimental points check the theoretical curve calculated for W_e in the case of Cu and C showing no large contributions to these reactions from high energy photons.

The slope of the transition curves at large absorber depths should correspond to the lowest energy photon participating in the reaction. This again is hard to measure accurately due to the low sample activity in this region. Also, contamination by neutron background is difficult to separate from the photon induced activity. The final slopes, before these effects become appreciable, correspond to 15 Mev and 18 Mev in the case of Cu and C detectors, in reasonable agreement with the known thresholds[2] of 10.9 Mev and 18.7 Mev.

---

* Evidence for photofission in Bi has recently been reported by N. Sugarman, Phys. Rev. 79, 532 (1950)

The effective reaction energy W_e as obtained from the track length is defined as follows:

$$W_e = \frac{\int_{W_{min}}^{W_o} W\ \sigma(W)\ Z(W)\ N(W)\ dW}{\int_{W_{min}}^{W_o} \sigma(W)\ Z(W)\ N(W)\ dW} \qquad (1)$$

where W = photon energy

$\sigma(W)$ = reaction cross section for photons of energy W

$Z(W)$ = track length of transition curve for photons of energy W produced in Pb by 322 Mev bremsstrahlung

W_o = quantum limit of the x-ray beam

W_{min} = threshold energy of the reaction

$N(W)$ = number of photons of energy W present in the incident beam.

In the case where the energies of the photons responsible for a given reaction are grouped around an average value as is believed to be the case for the reaction studied here, the value of W_e is close to the average energy as shown in detail by Eyges.[6]

The main advantages of the track length method of determining the average energy W_e of the photons responsible for certain nuclear reactions are as follows:

(1) No beam monitor with an accurately known energy dependence is required.

(2) For long half-lives, only one bombardment is needed to obtain the effective energy. This is important since the irradiation times are of the order of a half-life.

(3) For short half-lives, few bombardments are needed to obtain a fair value for W_e. This is useful in the case of new activities.

The main disadvantage of the method comes from the absence of detailed information on the shape of the excitation functions.

III. Integrated Reaction Cross Section and Relative Yields

A. Method. When a target is placed in the synchrotron beam, the number of reactions n per unit time of bombardment is given by:

$$n = N \int_{W_{min}}^{W_o} \sigma(W)\, dq\,(W) \qquad (2)$$

where N = number of target nuclei per unit area

dq(W) = number of photons of energy between W and W + dW incident on the target per unit time.

The other symbols have the same meaning as in Equation (1). This expression will now be transformed in terms of quantities that can be calculated or measured.

The energy spectrum of the synchrotron beam as calculated for 321 Mev electrons incident normally on a 0.020 inch platinum target is shown in Fig. 7. The ordinate represents a function f(W) given by the equation

$$q(W)\, dW = k\, f(W) \frac{dW}{W} \qquad (3)$$

The numerical value of the constant k is equal to U, the energy incident on the target per unit time, as can be seen as follows. The numerical value of the ordinate of Fig. 7 has been chosen so that the area under the curve is unity. This means that

$$U = \int_0^{322} W\, q(W)\, dW = k \int_0^{322} f(W)\, dW = k$$

The variation of f(W) with energy takes into account the deviation of the

beam spectrum as calculated for the Berkeley synchrotron from the expression $\frac{dW}{W}$.

Equation (3) now becomes:

$$n = NU \int_{W_{min}}^{W_o} \sigma(W) \frac{f(W)}{W} dW \qquad (4)$$

If $\sigma(W)$ has an appreciable value only near the effective energy W_e this can be written

$$n = NU \frac{f(W_e)}{W_e} \int_{W_{min}}^{W_o} \sigma(W)\, dW = NU \frac{f(W_e)}{W_e} \sigma_{int} \qquad (5)$$

To obtain the integrated cross section σ_{int} of a reaction, it is thus necessary to measure n, U and W_e. The transition curve method is well suited to obtain this last quantity.

In practice, the yield y_1 of a reaction 1 is often measured with respect to the yield y_2 of a reaction 2. The relative cross section can then be calculated using

$$\frac{\sigma_1}{\sigma_2} = \frac{W_e^1}{W_e^2} \frac{f(W_e^2)}{f(W_e^1)} \frac{y_1}{y_2} \qquad (6)$$

B. Integrated Cross Section. σ_{int} has been measured for the reactions $C^{12}(\gamma,n)C^{11}$ and $Cu^{63}(\gamma,n)Cu^{62}$ and the results as calculated with Equation (5) are given in Table III. The values of W_e as obtained from the transition curves were used.

The energy U incident on the target per unit time was measured by a method developed by Blocker, Kenney and Panofsky which is described in detail elsewhere.[12] Only the procedure as applied to this particular problem will

[12] W. Blocker, R. W. Kenney, and W. K. H. Panofsky, Phys. Rev. 79, 419 (1950)

be outlined. The set-up consists of a monitor ionization chamber, a two inch collimator and a large ionization chamber of known geometry placed in the beam respectively at 4 feet, 4 3/4 feet, and 5 3/4 feet from the platinum target. A thin polystyrene sample holder was situated on the front face of the large chamber so that sample disks could be irradiated under repeatable geometrical conditions.

The monitor chamber was calibrated* against the beam energy passing through the selected target area by the use of Pb, Cu and Al disks of the same (7/8 in.) diameter and containing the same number of electrons. The taking of Pb-Al and Pb-Cu ionization current differences eliminates effects due to background and Compton electrons. It is then possible to calculate[12] the energy passing through the target area per unit current in the monitor ionization chamber. Cu and C disks of 7/8 in. diameter were then irradiated in the standard area. U is obtained from the integrated beam as measured by the calibrated monitor chamber. The number of reactions n per unit time of bombardment is calculated by the usual method from the number of counts obtained by placing the sample under an end window Geiger counter. Beam intensity variation, length of bombardment, decay during and after irradiation, sample self absorption and counter efficiency** are all taken into account.

The accuracy of the values of σ_{int} is estimated to be 25 percent. The result for the $Cu^{63}(\gamma,n)Cu^{62}$ reaction is in fair agreement with the value reported by Katz et al. (0.6 Mev-barns with 25 Mev betatron). The integrated cross section for $C^{12}(\gamma,n)C^{11}$ is lower than the value obtained by Lawson and Perlman (0.15 Mev-barns with 100 Mev betatron) but the discrepancy does not

---

* The author is indebted to W. Blocker and R. Kenney for this calibration.

** The absolute β standard used consists of a thin U_3O_8 deposit covered with an Al foil. The calibration by coincidence methods was done by L. Aamodt. The Cu and C disks and the U_3O_8 deposit were of approximately equal size.

lie outside the estimated errors.

C. Relative Yields. It is of interest to know the relative yield of several photonuclear reactions starting from one element. Zn was chosen for such a study because of the relatively convenient half-lives and known decay schemes of several product nuclei. The results are summarized in Table II and represent the average of two or more measurements. Where W_e is known, the relative cross sections are calculated using Equation (6). The yield of the reaction $Cu^{63}(\gamma,n)Cu^{62}$ is taken as unity since the yield of the 10.1 minute activity of Cu^{62} was usually used as a reference.

To obtain the relative yield of reactions leading to different product nuclei, the activities as extrapolated to the end of the bombardment were used after the following factors had been taken into account: counting efficiency from decay scheme, self-absorption, decay during irradiation, and beam intensity variation. This last factor was obtained by numerical integration of the beam intensity as recorded by the monitor ionization chamber.

Low induced activity presented the main difficulty in these measurements. Except for some (γ,n) and (γ,pn) reactions, the use of thin samples with negligible self-absorption proved impractical. Thick samples can be used in the x-ray beam, the maximum allowable thickness being determined by the transition curves corresponding to the reactions under study. However, the self-absorption of the radiation from the product nuclei then becomes important. This was taken into account in three ways:

(1) Cu was separated with small amounts of carrier after bombardment of thick $ZnSO_4$ samples; the activity of the resulting thin Cu sample was followed to obtain the relative yields of Cu^{61}, Cu^{64} and Cu^{67} with respect to Cu^{62}.

(2) Isotopically enriched samples of ZnO* were used to obtain the yields

* Supplied by the Carbide and Carbon Chemicals Corporation.

of Cu^{61}, Cu^{62} and Zn^{63} from the various Zn isotopes by counting samples of identical thickness and area.

(3) Since Zn^{62} decays 90 percent by K capture and the counter efficiency for x-rays is very low, nearly the same radiation is counted from Zn^{62} and Cu^{62}: The relative yield can therefore be obtained from a thick sample.

The uncertainty of the given results varies with the different reactions, but is estimated to be less than 30 percent.

D. Summary. A lower limit to the total integrated cross section σ_{int}^{total} for photon absorption by the Zn nucleus can be estimated from the results summarized in Table II since $\sigma_{int}^{total} = \sum \sigma_{int}$. This sum should be extended over all possible reactions to give the correct value. Adding the integrated cross sections, for the (γ,n), $(\gamma,2n)$, (γ,p), (γ,pn) and $(\gamma,p2n)$ reactions, a value of 1.2 Mev-barns is obtained. The relative yields, but not W_e, are known for the $(\gamma,3n)$, $(\gamma,p3n)$ and $(\gamma,p4n)$ processes. By estimating the corresponding effective photon energies from the number of ejected nucleons, an additional contribution of about 0.2 Mev-barns is obtained. The fact that not all of the observed reactions started from the same Zn isotope should not greatly affect this result since the excited nuclei were all of the even-even type. Thus we obtain

$$\sigma_{int}^{total} \geqslant 1.4 \text{ Mev-barns}$$

In a similar manner a lower limit for the mean energy $\overline{W}$ for photon absorption can be estimated using $\overline{W} = \sum \sigma_{int} W_e / \sum \sigma_{int}$. The result is

$$\overline{W} \geqslant 30 \text{ Mev}$$

It should be noted that the relative yields of the (γ,n) reactions observed with 322 Mev bremsstrahlung agree well within experimental errors with the G. E. results obtained with 100 Mev and 50 Mev betatron beams.

IV. Conclusions

From the results reported in this paper it is apparent that the (γ,n) process is the dominant mode of decay of the x-ray excited Zn nucleus. However other reactions contribute at least an equal amount to the total absorption cross section. It thus appears that the photon absorption curve has a broad maximum around 20 Mev, tailing off slowly at higher energies.

In a recent paper Levinger and Bethe[13] show from quite general sum rule considerations that photon absorption by dipole transitions leads to a reasonable total absorption cross section if exchange forces are included. The results reported here agree well with their calculations, since the value of x (the fraction of the n-p interaction due to exchange force) obtained from $\sigma_{int}^{total} = 1.4$ Mev-barns and $\overline{W} = 30$ Mev is of the correct order of magnitude.

Goldhaber and Teller[14] have proposed a more specific model for nuclear dipole absorption in which only one excited level is of importance. This leads to sharp resonance absorption and scattering. The importance of processes resulting in the ejection of more than one nucleon seems to indicate that at least some other process for higher energy photon absorption must exist.

The decay of the compound nucleus Zn^{64} when excited by different methods is of interest. Ghoshal[15] has obtained this compound nucleus by α-particle bombardment of Ni and proton bombardment of Cu, while in this paper the excitation with x-rays has been described. The cross section for formation of the compound nucleus depends of course on the method of excitation, but the decay might be independent of this factor if the nucleus has lost all "memory" of its origin. Ghoshal finds the peak of the (γ,n) reaction at 20 Mev, the peaks of the $(\gamma,2n)$

---

13 J. S. Levinger and H. A. Bethe, Phys. Rev. 78, 115 (1950)

14 M. Goldhaber and E. Teller, Phys. Rev. 74, 1046 (1948)

15 S. Ghoshal, Phys. Rev. (in press)

and (γ,pn) processes at 31 Mev. The values of W_e for the reaction (γ,n), (γ,2n) and (γ,pn) are 19 Mev, 29 Mev and 30 Mev respectively. This close agreement is not suprising since the α-particle binding energy is small. In addition Ghoshal finds that the yield of the (α or p,pn) reaction is four times larger than the yield of the (α or p,2n) process. The relative yield of 5.5 of the corresponding x-ray induced reactions is quite similar considering that peak and integrated cross sections are being compared. It thus appears that the decay of a 30 Mev excited Zn nucleus does not depend on its method of excitation.

Levinthal and Silverman[16] have obtained energy and angular distributions of protons emitted by several elements irradiated in the synchrotron beam. They find a relatively large number of high energy protons that would not be expected according to the statistical theory, and these protons show an asymmetrical angular distribution. This indicates that the (γ,p) reaction is not necessarily produced by photons grouped in a narrow interval around W_e. This should be noticeable from the shape of the transition curve corresponding to the (γ,p) reaction. It is unfortunate that the accuracy obtained in this case does not warrant any conclusions along this line.

It is a pleasure to thank Professor A. C. Helmholz under whose guidance this work was carried out for many helpful suggestions and assistance, and Professor E. McMillan for his constructive interest and support. Several conversations with Professor R. Serber on the interpretation of the transition curves proved very fruitful. The author is very much indebted to Dr. L. Eyges for taking an interest in this problem and performing the required calculations. Mr. J. Rose assisted in some of the measurements and his help is much appreciated. Finally this work would not have been possible without the fine cooperation

---

16 C. Levinthal and A. Silverman, Phys. Rev. (in press)

of Mr. W. Gibbins, Mr. G. McFarland and the synchrotron crew.

This work was sponsored by the U. S. Atomic Energy Commission.

Information Division
scb/10-11-50

Table I

Experimental and theoretical track length ratios

for 322 Mev and 200 Mev bremsstrahlung

Reaction	Beam Energy (Mev)	Observed Track Length	Ratio Exp.	Ratio Theor.
$C^{12}(\gamma,n)C^{11}$	322	6.43	1.44	1.50
	205±5	4.48		
$Cu^{63}(\gamma,n)Cu^{62}$	322	10.0	1.51	1.55
	201±5	6.63		

Table II

Effective photon energy W_e, relative yields and integrated cross sections for some nuclear reactions induced by 322 Mev bremsstrahlung

Reaction	Product Half-life	Product β-particles and Energy(Mev)[a]	Track Length (radiation length)	W_e (Mev)	Relative Yield	Relative σ_{int}
$C^{12}(\gamma,n)C^{11}$	20 min.	β^+ 0.99	6.4	27	0.074	0.12
$Cu^{63}(\gamma,n)Cu^{62}$	10.1 min.	β^+ 2.92[b]	10.0	18	1.0	1.0
$Cu^{65}(\gamma,n)Cu^{64}$	12.8 hrs	β^+ 0.64 (15%) β^- 0.57 (31%) K (54%)		19[d]	1.2	1.3
$Zn^{64}(\gamma,n)Zn^{63}$	38 min.	β^+ 0.47(1%); 1.40(7%); 2.36(85%) K (7%)	9.3	19	0.83	0.89
$Zn^{68}(\gamma,p)Cu^{67}$	63 hrs.	β^- 0.56	7.2	24	0.070	0.097
$Zn^{64}(\gamma,2n)Zn^{62}$	9.5 hrs.	β^+ 0.66 (10%)[b] K (90%)	5.9	29	0.039	0.067
$Zn^{64}(\gamma,pn)Cu^{62}$	10.1 min.	see above	5.5	30	0.21	0.37
$Zn^{66}(\gamma,pn)Cu^{64}$	12.8 hrs.	see above		30[d]	0.11	0.19
$Zn^{66}(\gamma,3n)Zn^{63}$	38 min.	see above			0.029	
$Zn^{64}(\gamma,p2n)Cu^{61}$	3.4 hrs.	β^+ 1.20(63%); 0.55(2.5%) 0.26 (0.03%)[c] K (34%)	2.9[d]	57[d]	0.045	0.17
$Zn^{67}(\gamma,4n)Zn^{63}$	38 min.	see above			<0.02	
$Zn^{66}(\gamma,p3n)Cu^{62}$	10 min.	see above			0.033	
$Zn^{66}(\gamma,p4n)Cu^{61}$	3.4 hrs.	see above			0.014	
$Ag^{107}(\gamma,n)Ag^{106}$	24 min.	β^+ 2.0 Mev	10.9	16		
$Ta^{181}(\gamma,n)Ta^{180}$	8 hrs.		9.3	19		
$Ta^{181}(\gamma,2p...)_{rare\ earth}$	70 min.	?	2.5	68		
$Pb(\gamma,?)$	hours	?	2.2	78		
$Pb(\gamma,?)$	days	?	2.9	57		
$Bi^{209}(\gamma,?)$	hours	?	2.2	78		

(a) Unless otherwise stated values taken from G. T. Seaborg and I. Perlman, Rev. Mod. Phys. 20, 585 (1948)

(b) R. W. Hayward, Phys. Rev. 79, 541 (1950)

(c) G. E. Owen, C. S. Cook and P. H. Owen, Phys. Rev. 78, 686 (1950)

(d) Only a few points were obtained for the transition curve, and W_e estimated by comparison with complete curves

Table III

Integrated Reaction Cross Sections

Reaction	W_e(Mev)	σ^{int}(Mev-barn)
$C^{12}(\gamma,n)C^{11}$	27	0.090
$Cu^{63}(\gamma,n)Cu^{62}$	18	0.76

Figure Captions

Fig. 1 Position of absorber stack with respect to the synchrotron and various geometries used in the experiment

Fig. 2 Influence of geometry on transition curve in Pb of x-rays causing the reaction $Cu^{63}(\gamma,n)Cu^{62}$

Fig. 3 Beginning of transition curves of x-rays responsible for several (γ,n) reactions

Fig. 4 Semi-logarithmic plot of transition curves of x-rays responsible for several (γ,n) reactions

Fig. 5 Semi-logarithmic plot of transition curves of x-rays responsible for several reactions from Zn taken with 322 Mev bremsstrahlung

Fig. 6 Semi-logarithmic plot of transition curves of x-rays responsible for several reactions from Ta, Pb and Bi taken with 322 Mev bremsstrahlung

Fig. 7 Theoretical bremsstrahlung spectrum from the Berkeley synchrotron. The function f(W) is defined by Equation (3). The ordinate scale is chosen to normalize the area under the curve to unity.

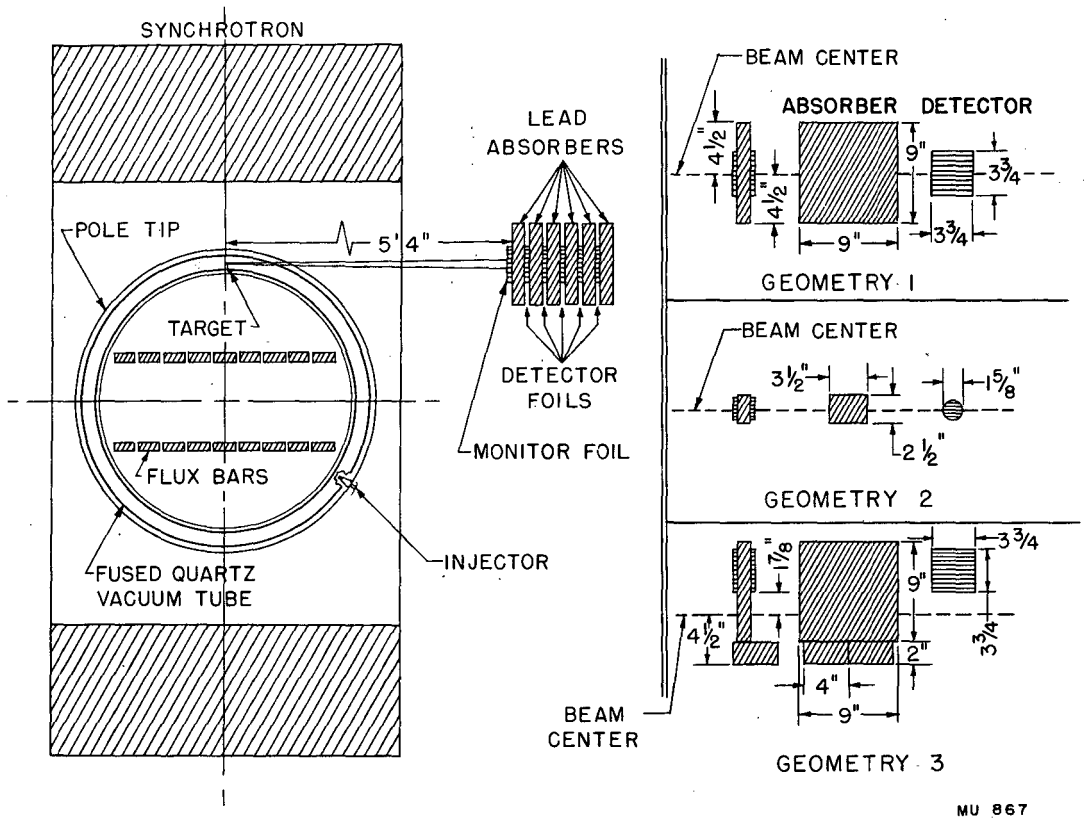
SYNCHROTRON
POLE TIP
5'4"
TARGET
FLUX BARS
FUSED QUARTZ
VACUUM TUBE
INJECTOR
LEAD
ABSORBERS
DETECTOR
FOILS
MONITOR FOIL
BEAM CENTER
ABSORBER DETECTOR
4½"
1"
4½"
9"
3¾
9"
3¾
GEOMETRY 1
BEAM CENTER
3½"
1⅝"
2½"
GEOMETRY 2
3¾
1⅞"
9"
4½"
2"
3¾
4"
9"
BEAM
CENTER
GEOMETRY 3
MU 867

Fig. 1

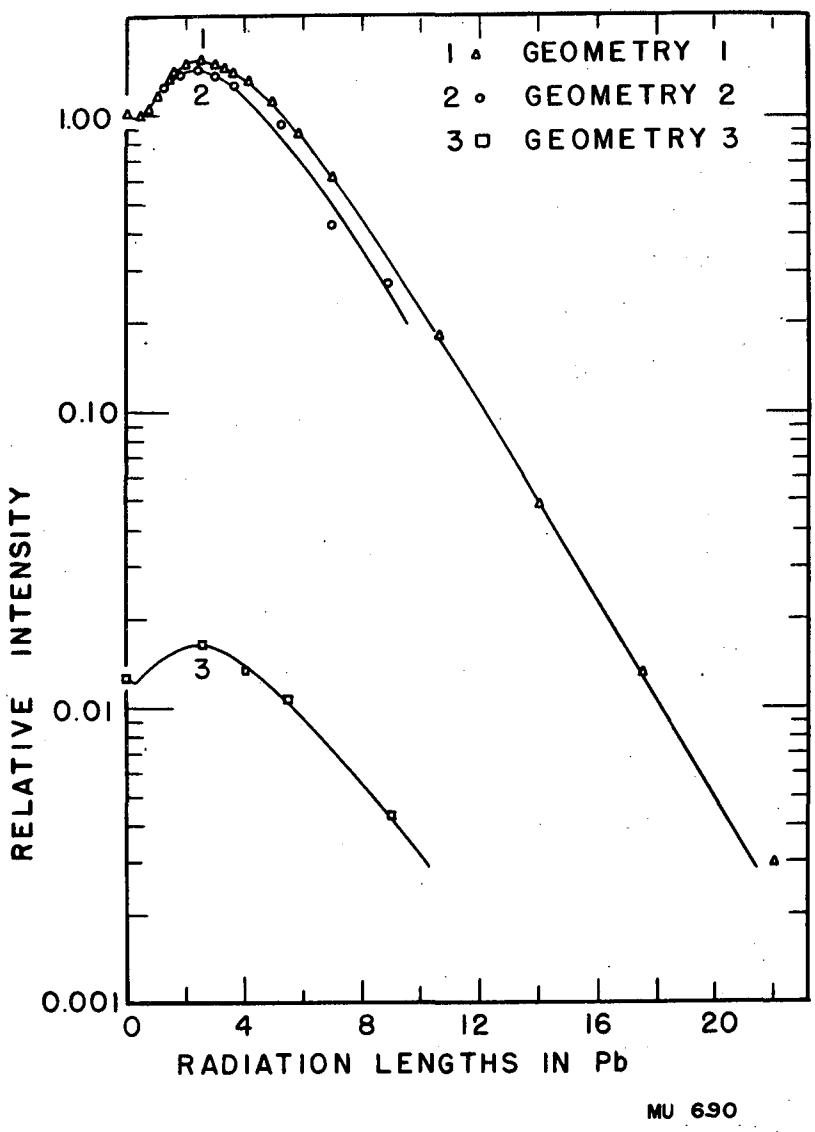
1 △ GEOMETRY 1
2 ○ GEOMETRY 2
3 □ GEOMETRY 3
1.00
0.10
0.01
0.001
RELATIVE INTENSITY
0
4
8
12
16
20
RADIATION LENGTHS IN Pb
MU 690

Fig. 2

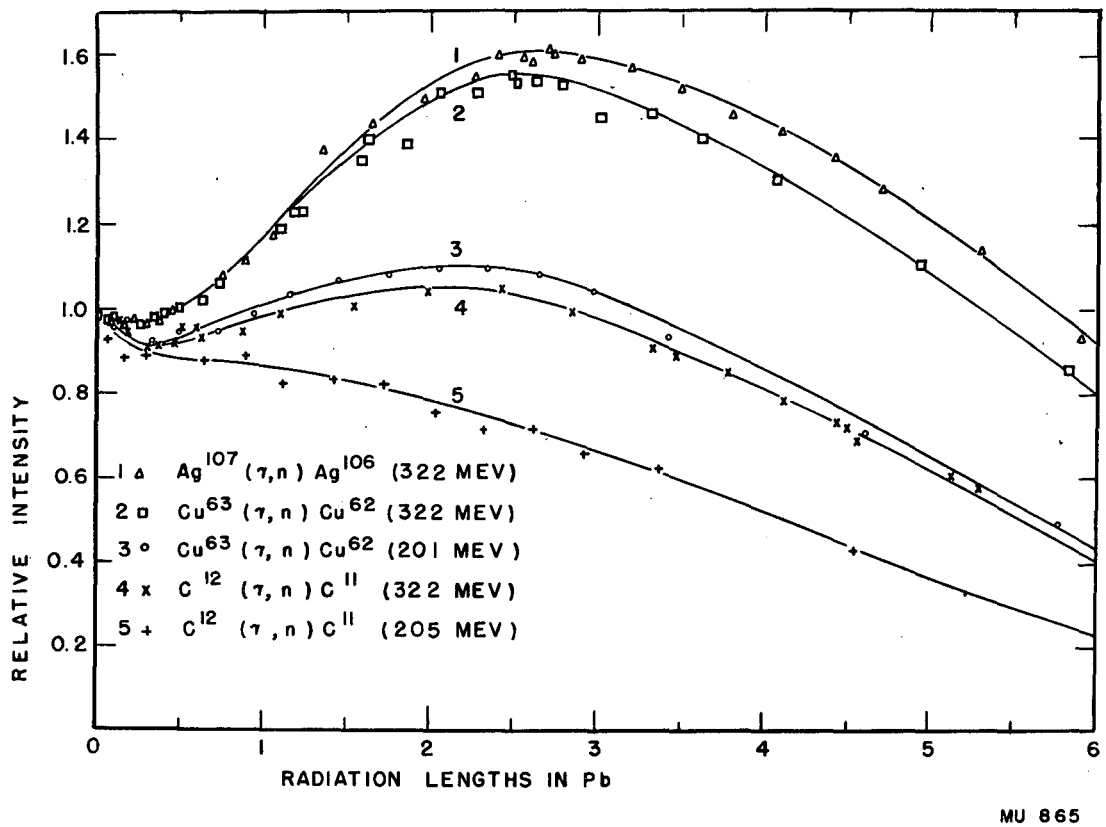
RELATIVE INTENSITY
RADIATION LENGTHS IN Pb
1 Δ Ag107 (γ,n) Ag106 (322 MEV)
2 □ Cu63 (γ, n) Cu62 (322 MEV)
3 ○ Cu63 (γ, n) Cu62 (201 MEV)
4 x C12 (γ, n) C11 (322 MEV)
5 + C12 (γ, n) C11 (205 MEV)
MU 865

Fig. 3

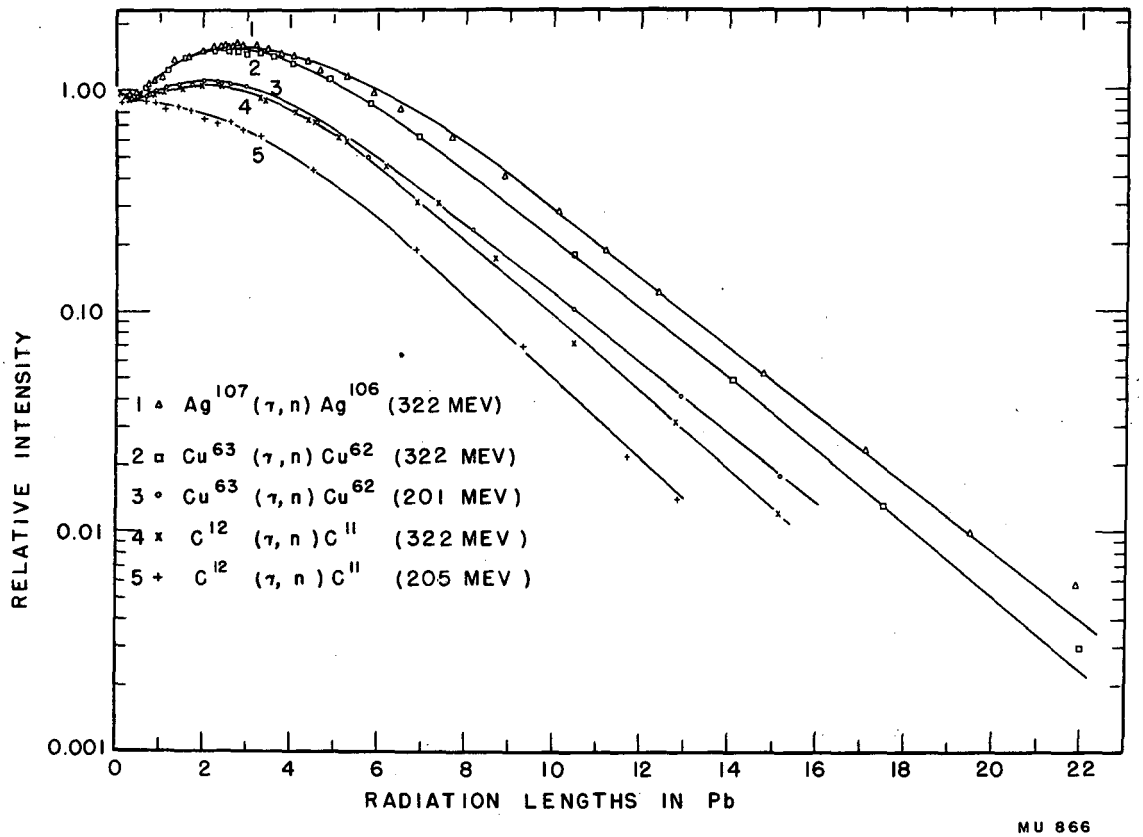
1.00
0.10
0.01
0.001
RELATIVE INTENSITY
0
2
4
6
8
10
12
14
16
18
20
22
RADIATION LENGTHS IN Pb
1 △ Ag107 (γ, n) Ag106 (322 MEV)
2 □ Cu63 (γ, n) Cu62 (322 MEV)
3 ○ Cu63 (γ, n) Cu62 (201 MEV)
4 × C12 (γ, n) C11 (322 MEV)
5 + C12 (γ, n) C11 (205 MEV)
MU 866

Fig. 4

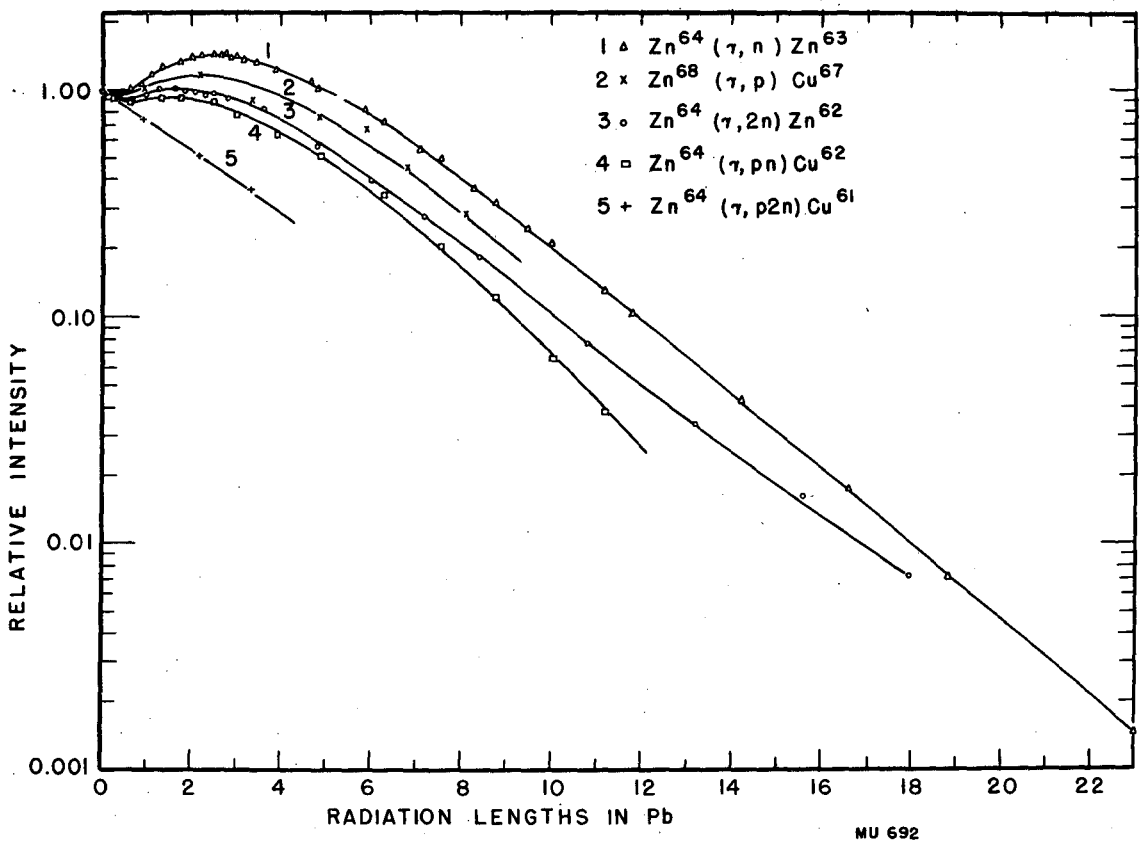
1 Δ Zn^{64} (γ, n) Zn^{63}
2 × Zn^{68} (γ, p) Cu^{67}
3 ○ Zn^{64} (γ, 2n) Zn^{62}
4 □ Zn^{64} (γ, pn) Cu^{62}
5 + Zn^{64} (γ, p2n) Cu^{61}
RELATIVE INTENSITY
1.00
0.10
0.01
0.001
0
2
4
6
8
10
12
14
16
18
20
22
RADIATION LENGTHS IN Pb
MU 692

Fig. 5

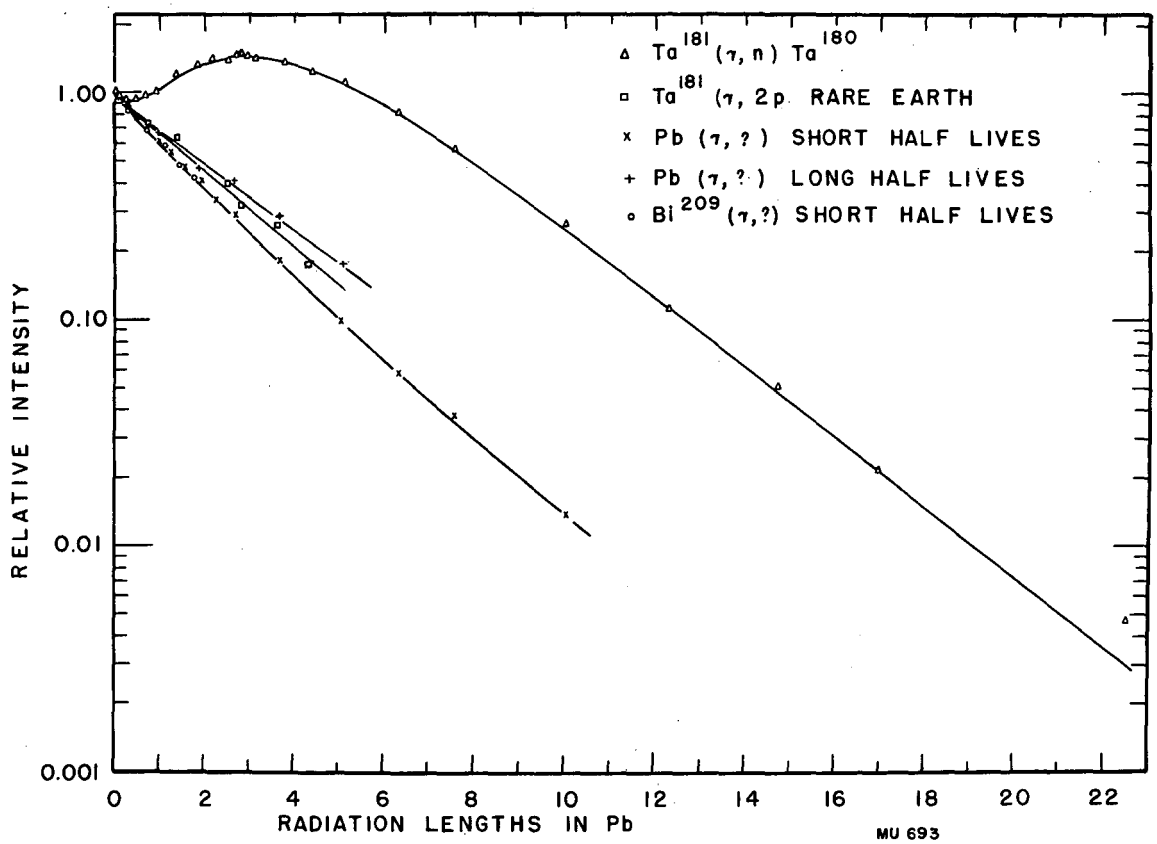
Ta 181 (γ, n) Ta 180
Ta 181 (γ, 2p RARE EARTH
Pb (γ, ?) SHORT HALF LIVES
Pb (γ, ?) LONG HALF LIVES
Bi 209 (γ,?) SHORT HALF LIVES
RELATIVE INTENSITY
1.00
0.10
0.01
0.001
0
2
4
6
8
10
12
14
16
18
20
22
RADIATION LENGTHS IN Pb
MU 693

Fig. 6

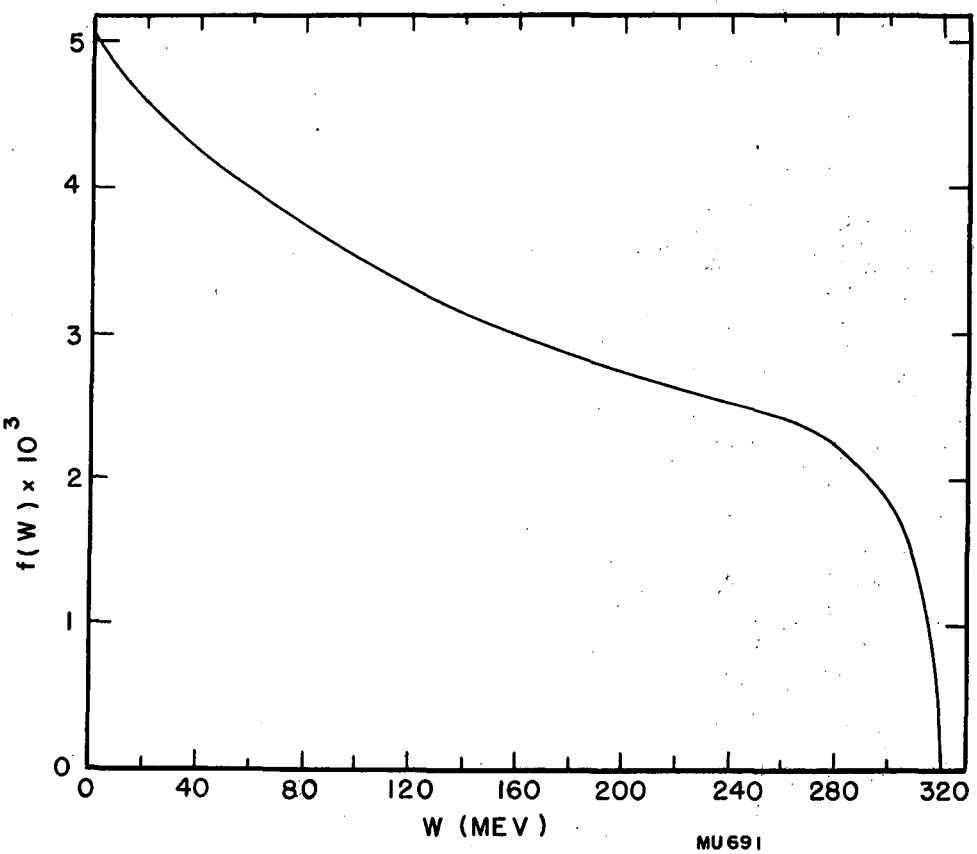

Fig. 7